20th International Conference on Structural Mechanics in Reactor Technology (SMiRT 20)
Espoo, Finland, August 9-14, 2009
SMiRT 20-Division 9, Paper 2012

Optical Strain Measurement of Plastic Strain Localization in Nuclear Waste Copper Canisters

Kati Savolainen, Tapio Saukkonen, and Hannu Hänninen

Department of Engineering Design and Production, Laboratory of Engineering Materials, Helsinki University of Technology, Espoo, Finland, e-mail: kati.savolainen@tkk.fi

Keywords: Copper, Weld, Plastic strain, Localization.

1 ABSTRACT

In Finland and Sweden the spent nuclear fuel will be stored in a deep repository in copper corrosion barrier canisters surrounding cast iron inserts. The 50 mm thick copper canisters will we sealed using either electron beam welding (EB) or friction stir welding (FSW) to join the tubes and the lids/bottoms. The canisters will deform in the repository conditions e.g. due to hydrostatic pressure. The deformation will localize to different discontinuities, such as defects and microstructural heterogeneity.

This study compared the localization of plastic deformation in EB and FSW welds as well as in the base materials (both forged and extruded) using optical strain measurement methods. The results show that in the base materials the deformation occurs very uniformly over the entire gauge length. In FSWelds the deformation localizes in the middle of the weld, however, the tensile strength is similar to that of the base materials. In EB welds the deformation localizes to the large grains in the middle of the weld and to the steep grain size gradient between the weld and the base material. Tensile strength is lowest in the EB welds (175 MPa as compared to 200 MPa or higher for the other samples).

2 INTRODUCTION

Finland and Sweden have decided that the spent nuclear fuel will be encapsulated and buried into long-term repositories. The spent fuel will be placed in cast iron inserts surrounded by copper corrosion barrier canisters. The 50 mm thick copper canisters consist of an extruded tubular body and forged lid and bottom parts. The canisters will be sealed using either electron beam welding (EB) or friction stir welding (FSW) to join the tubes and the lids/bottoms. Plastic deformation caused by the repository conditions, such as hydrostatic pressure and bentonite swelling, will not be distributed evenly around the canister, but instead it will concentrate in certain locations. Microstructural defects, geometric discontinuities, as well as microstructural heterogeneity and residual stresses of the welds, in particular, localize plastic deformation.

The aim of this study is to determine where the plastic deformation localizes in the different parts of the copper canister. An optical strain measurement system was used to measure and analyze the deformation of the samples. The system records successive images of the sample surface and constructs the deformation field using advanced cross correlation algorithms.

The amount of residual plastic strain is known to have an effect on different long-term materials properties. For instance, Wilshire and Palmer (2004) showed the effect of prestrain (dislocation density) on creep of copper. In austenitic AISI 304 stainless steel the amount of cold work exceeding 20% is known to result in initiation of the stress corrosion cracking (Ehrnstén et al. 2001). Thus, when wanting to ascertain and evaluate the integrity of the copper canister it is very important to know the material properties even in very small localized areas. Electron backscatter diffraction (EBSD) and electron microscopy have in recent years proved to be a promising method to study the plastic strain and other material properties in localized areas. However, due to time constraint when wanting to map large areas, it is beneficial to be able to concentrate only on critical areas. The weld areas are typically exhibiting large variations of residual plastic strain and various discontinuities in the material properties. The optical strain measurement using large test

samples containing the whole weld area is an ideal method to detect the critical areas, which can later be studied with electron microscopy in detail.

Different manufacturing and welding methods result in different microstructures. Forged and extruded base materials have a small grain size. FSW is a solid state welding method, where the resulting microstructure has a small, equiaxed grain size, similar to those of the base materials. Properties of the FSWelds have been reported to be very close to those of the base materials (Cederqvist 2004). EB is a fusion welding method where a beam of high-energy electrons locally heats the material to a high temperature. The resulting microstructure has a very coarse grain size.

3 EXPERIMENTAL

The base materials of the forged lids and extruded tubes were slightly different depending on the manufacturing method (Table 1). Therefore, the base materials for the welds were different. Due to their similarity and restrictions in the amount of available material, optical strain measurements were made only with tube material of EB weld and lid material of the FSWeld. The samples were electro-discharge machined.

Table 1. Grain sizes and amount of twin boundaries of the total amount of grain boundaries of the base materials.

	Grain size (µm)				Twins (%)
	Horizontal		Vertical		
	Disregarding twins	Including twins	Disregarding twins	Including twins	
Tube (EB)	63	28	44	19	58
Tube (FSW)	75	32	76	35	60
Lid (EB)	70	39	52	30	30
Lid (FSW)	61	29	62	31	53

Tensile testing was performed by MTS 810 material test system at a constant rate of 0.02 mm/s using flat tensile samples. Welds were located at the centre of the gauge length of the specimens. Deformation fields were determined using StrainMaster optical strain measurement system by LaVision. Sample preparation for EBSD was made using SiC grinding papers, diamond polishing up to 1 µm, and electrolytic polishing. Zeiss Ultra 55 FEG-SEM and Channel5 acquisition and analysis software by HKL Technologies were used in SEM and EBSD studies. For macroscopic studies the samples were etched using 50%/50% solution of distilled water and nitric acid for 60 s.

4 RESULTS

Figure 1 shows a macrograph of the transverse section of an FSWeld. Figure 2 shows a macrograph of the transverse section of an EB weld. Figure 3 shows a longitudinal section of an EB weld exhibiting its very large grain size.

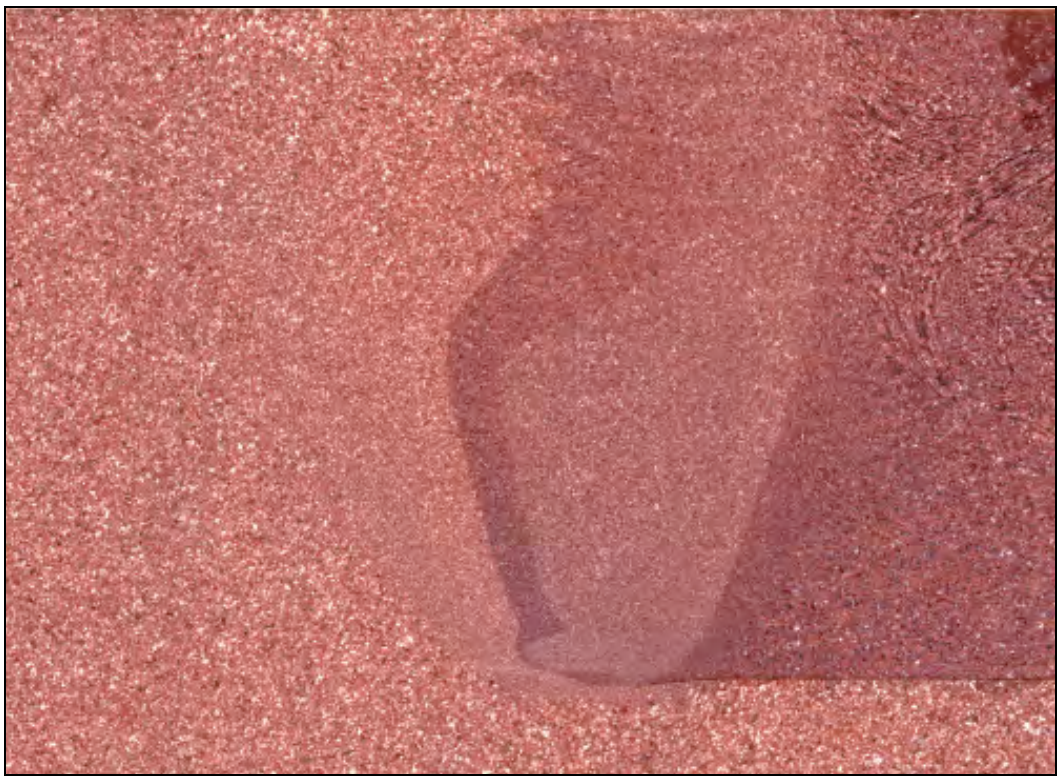

Figure 1. Macrograph of the transverse section of an FSWeld. Tube material is on the right side and lid material on the left side. Different zones of the weld can be clearly seen.

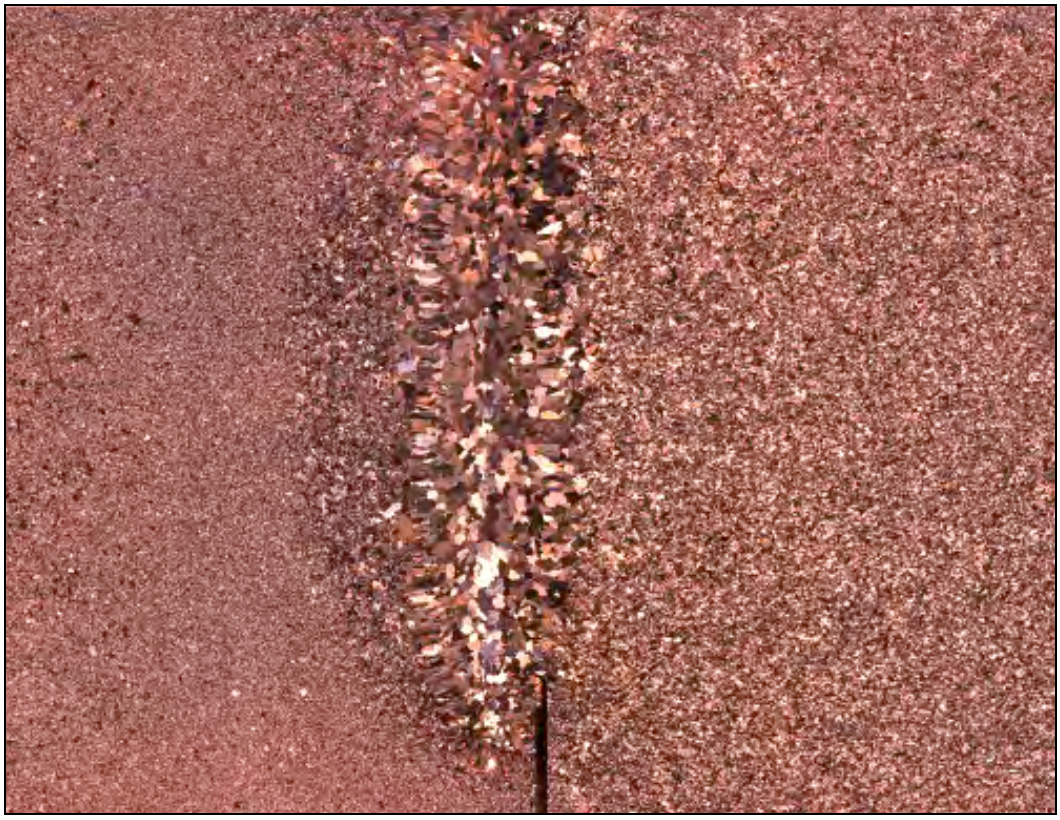

Figure 2. Macrograph of the transverse section of an EB weld. Tube material is on the left side and lid material on the right side. The large grain size of the weld can be clearly seen.

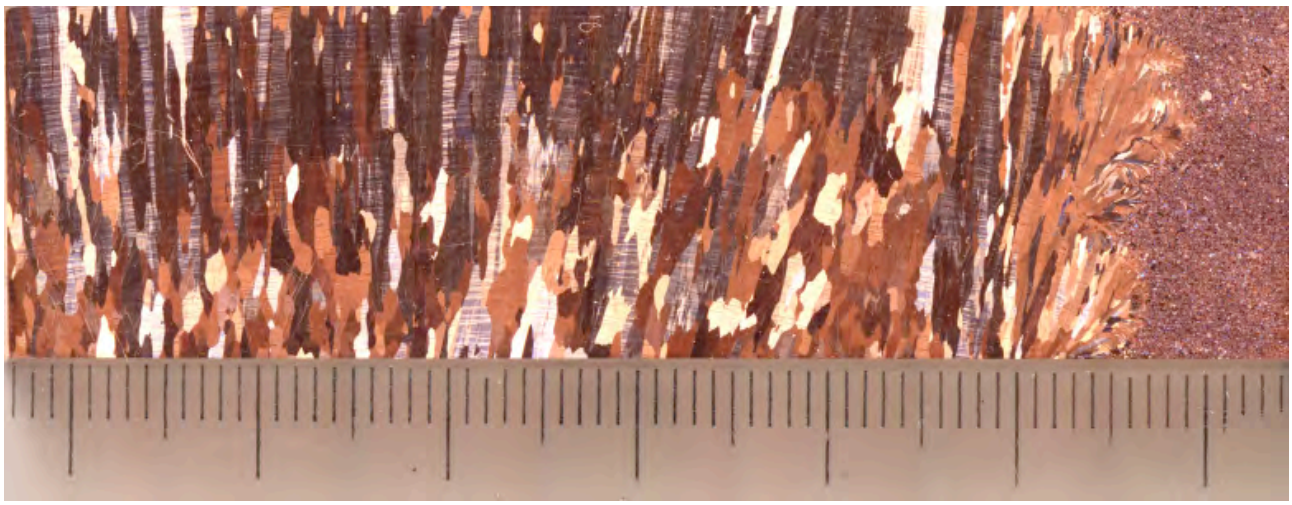

Figure 3. Macrograph of the longitudinal section of an EB weld. Top of the weld is on the left side and bottom on the right side. Tube material can be seen on the right side. The very large longitudinal grain size of the weld can be clearly seen.

Figure 4 shows a stress-strain curve for each sample type. It can be seen that the tensile strength of the EB weld is lower than that of the other samples. Tensile strength of the EB weld is 175 MPa while the other samples have a tensile strength of 200 MPa or higher. The extruded tube material has the highest tensile strength of 210 MPa.

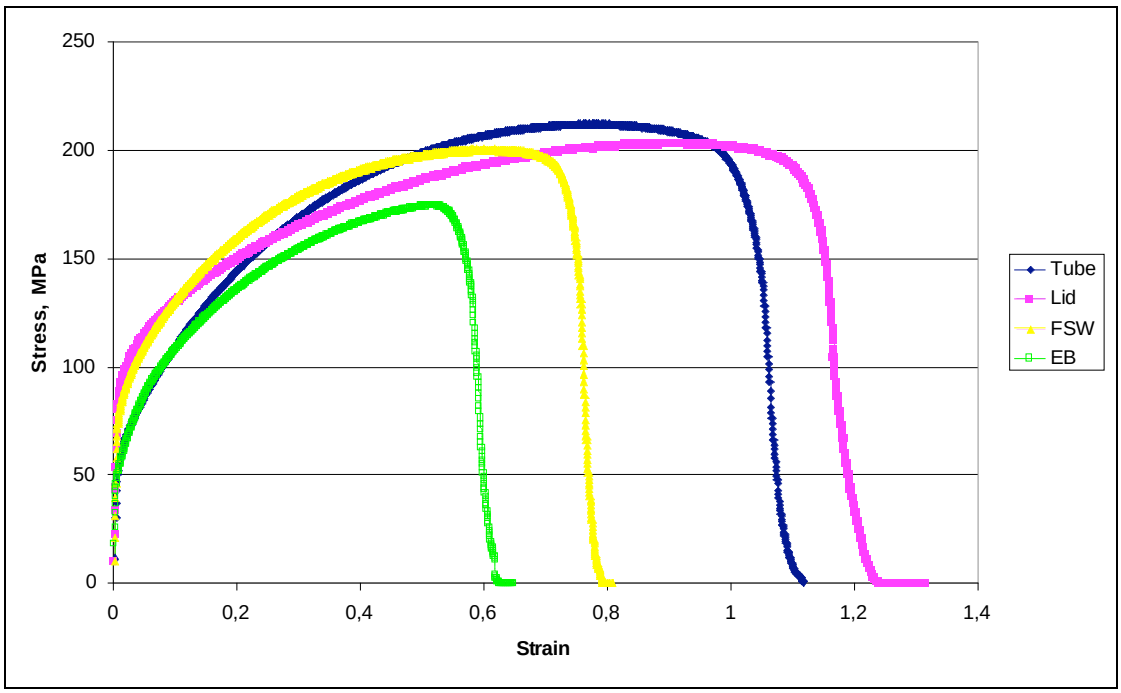

Figure 4. Stress-strain curves of each sample type. It can be seen that the tensile strength of the EB weld is low compared to that of the other samples, 175 MPa as compared to 200 MPa or higher of the other samples.

Uniform, local, and total strains of the samples can be seen in Table 2. Elongation to fracture is fairly similar with the forged and extruded base materials. However, for the FSWeld it is reduced by about one third and with the EB weld to half of the value for the base metals. The reduction of local strain with the EB weld is even more marked, being 60%.

Reduction of area of the samples was 90% for the base materials and 85% for the FSWeld. For EB weld the reduction of area varied depending on the fracture location. It was 85% when fracture occurred between the weld and the base material and 80% when fracture occurred in the middle of the weld.

Table 2. Uniform, local, and total strain of the samples.

	Uniform strain	Local strain	Total strain
Tube	0.84	0.28	1.12
Lid	0.91	0.32	1.23
FSW	0.61	0.17	0.79
EB	0.50	0.13	0.63

Figures 5-8 show the results of the optical strain measurements in Y-direction at the point of fracture. All images have the same scale for strain (0-5.0). All samples exhibit similar uniform elongation with the exception of the EB weld. In EB weld the extruded tube material is elongated much more than the forged lid material.

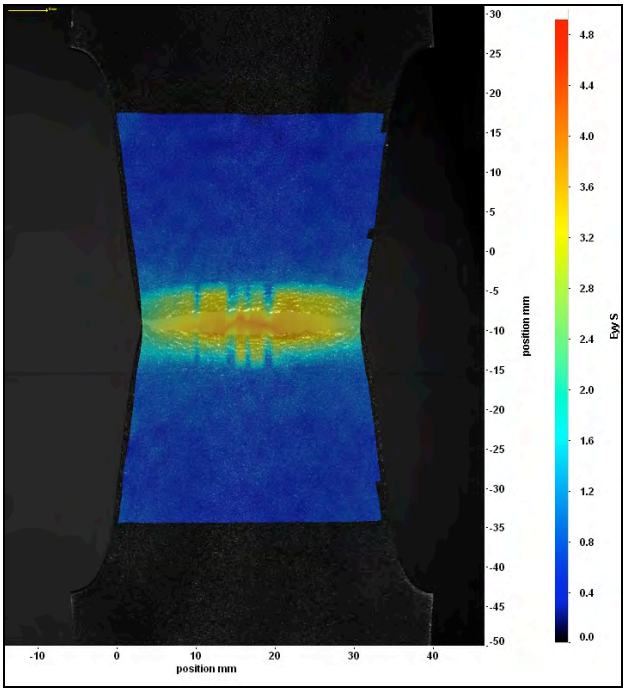

Figure 5. Strain map of lid material.

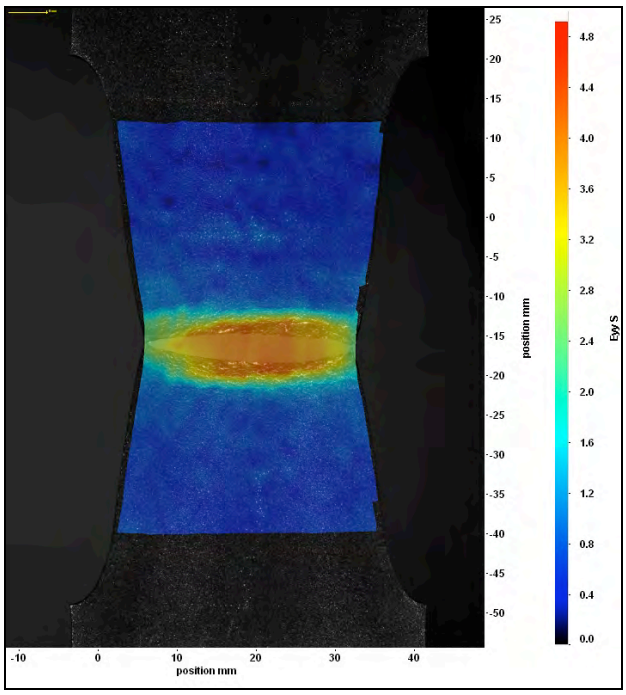

Figure 6. Strain map of tube material.

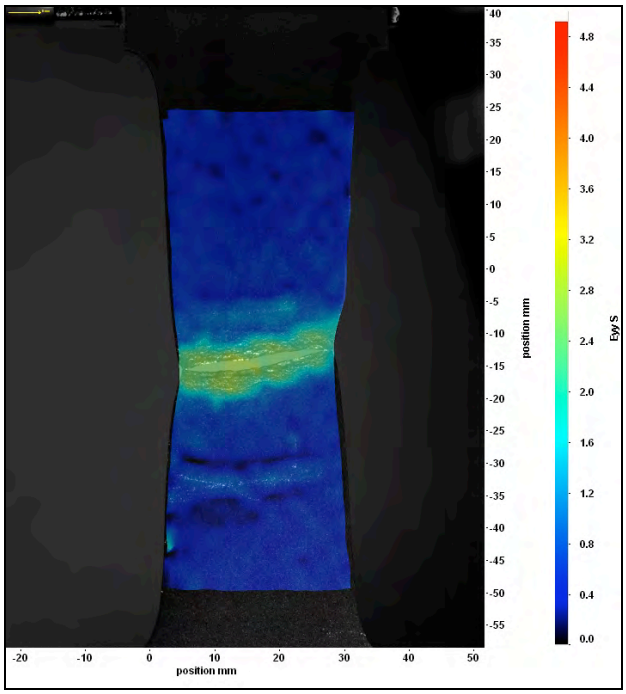

Figure 7. Strain map of an FSWeld. Tube material is on the top and lid material on the bottom. The fracture occurs between the weld and the lid material.

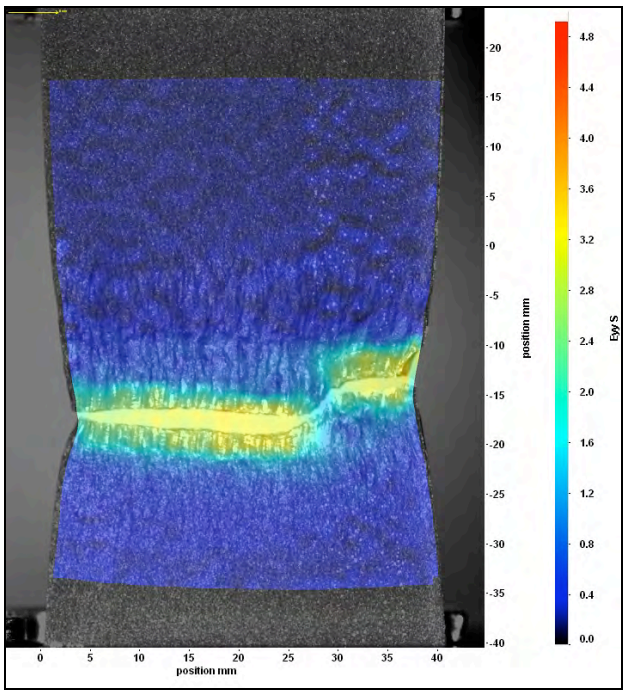

Figure 8. Strain map of an EB weld. Tube material is on the top and lid material on the bottom. Deformation localizes to the middle of the weld with large grain size as well as between the weld and the forged lid material due to large grain size gradient. It can also be seen that the extruded tube material is elongated much more than the forged lid material.

Figure 9 shows an EB weld after fracture. The fracture between the weld and the forged lid material can be clearly seen. Some strain localization has occurred in the middle of the weld and less between the weld and the extruded tube material.

Figure 9. EB weld after tensile testing. The weld has fractured between the weld and the forged lid material due to large grain size gradient. Deformation has also localized at the weld centre with large grains and slightly also between the weld and the extruded tube material where the grain size gradient is less dramatic.

Figure 10 shows an EBSD map of the root of an FSWeld. Part of the original joint line can be seen on the upper left corner of the image. Weld material is on the top and forged lid material is on the bottom. The smooth transition from the base material to the weld can be seen.

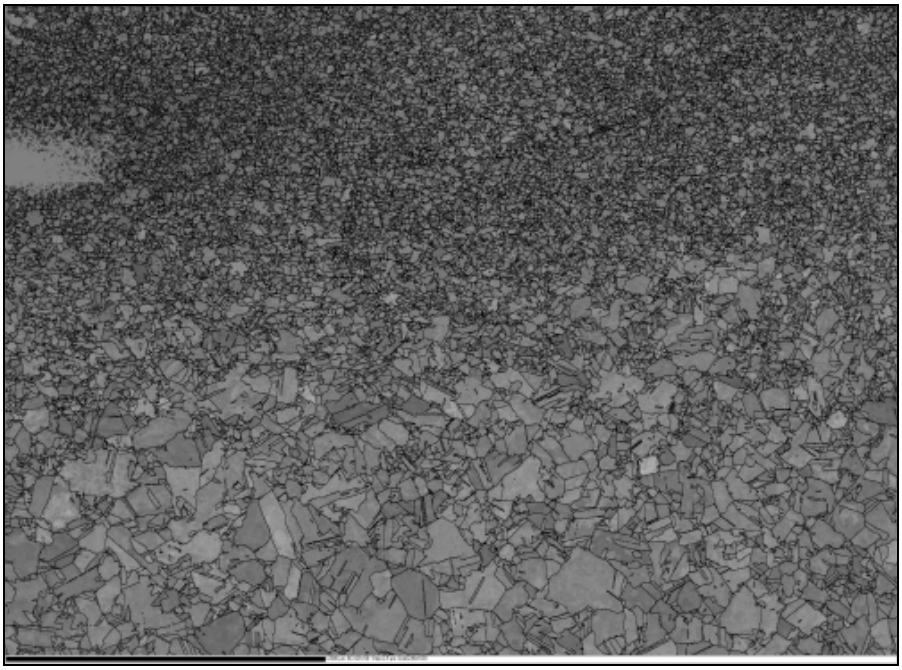

Figure 10. An EBSD map of the root of an FSWeld in transverse direction. Part of the original joint line can be seen on the upper left corner. The weld is on the top and forged lid material on the bottom. The transition from the weld to the base material is smooth.

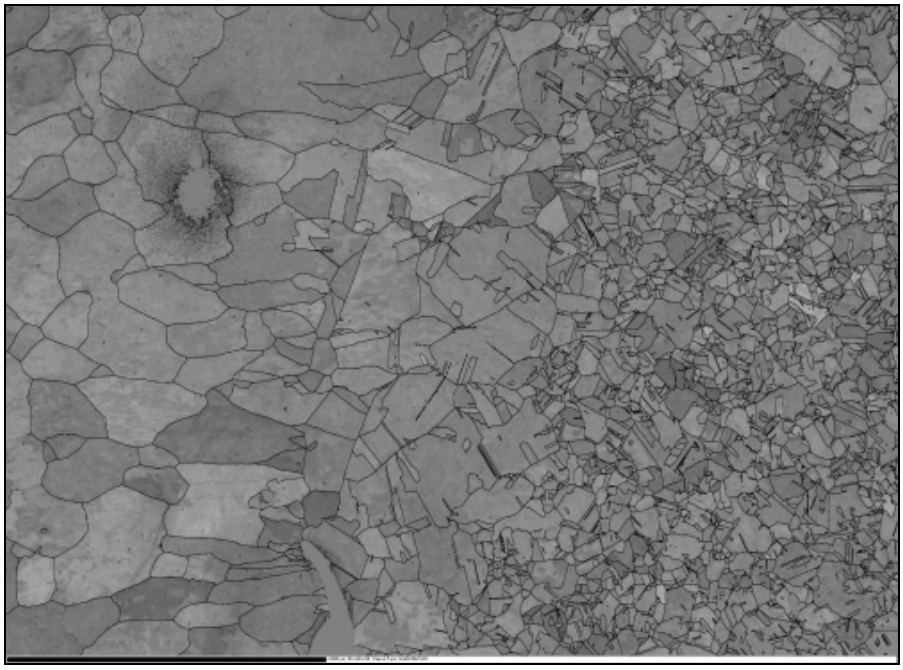

Figure 11. An EBSD map of the root of an EB weld in transverse direction. Part of the original joint line can be seen at the bottom, left from the centre. The weld is on the left and forged lid material on the right. The transition from the weld to the base material is abrupt and in the longitudinal direction the grain size gradient is even more pronounced. A weld defect (void) can be seen on the upper left corner.

5 CONCLUSION

Based on the results obtained in this study it can be concluded that deformation occurred quite uniformly in all the samples except for the EB weld. In EB welds the deformation localizes mainly to the large grains in the middle of the weld or at the fusion line between the lid and the EB weld due to the very steep grain size gradient. It was also noticed that in EB welds the extruded tube material is elongated more than the forged lid material. The tensile strength for EB weld was lower than that for the other materials, 175 MPa and 200 MPa or higher, respectively.

It needs to be noted that the strain rates used in this study are very high compared to the real strain rates during the 100 000 years in the repository. The actual strain rates are comparable to those of creep. The strain localization at extremely low strain rates combined with elevated temperatures will be significantly higher than that presented in this study, and this will be carefully studied in the future.

Acknowledgements. *The authors wish to thank SKB for FSWelds, Posiva for EB welds, and Kim Widell for help in tensile testing.*

REFERENCES

Cederqvist, L. 2004. FSW to Seal 50 mm Thick Copper Canisters – A Weld that Lasts for 100,000 Years. 5th International Friction Stir Welding Conference. Metz, France, 14-16 September. 6 p.

Ehrnstèn, U., Aaltonen, P., Nenonen, P., Hänninen, H., Jansson, C., and Angeliu, T. 2001. Intergranular Cracking of AISI 316NG Stainless Steel in BWR Environment. 10th Symposium on Environmental Degradation of Materials in Nuclear Power Systems – Water Reactors. Nevada, USA, 5-9 August. 10 p.

Wilshire, B. and Palmer, C.J. 2004. Strain Accumulation During Dislocation Creep of Prestrained Copper. Materials Science and Engineering. Vol. A:387-389. P 716-718.